# Prion Protein Selectively Binds Copper(II) Ions†

Johannes Stöckel,‡,⊥ Jiri Safar,‡ Andrew C. Wallace,§ Fred E. Cohen,§,|| and Stanley B. Prusiner*,‡,||

*Departments of Neurology, Biochemistry and Biophysics, and Cellular and Molecular Pharmacology, University of California, San Francisco, California 94143-0518*

*Received November 18, 1997; Revised Manuscript Received February 25, 1998*

ABSTRACT: The infectious isoform of the prion protein ($PrP^{Sc}$) is derived from cellular PrP ($PrP^{C}$) in a conversion reaction involving a dramatic reorganization of secondary and tertiary structure. While our understanding of the pathogenic role of $PrP^{Sc}$ has grown, the normal physiologic function of $PrP^{C}$ still remains unclear. Using recombinant Syrian hamster prion protein [SHaPrP(29−231)], we investigated metal ions as possible ligands of PrP. Near-UV circular dichroism spectroscopy (CD) indicates that the conformation of SHaPrP(29−231) resembles $PrP^{C}$ purified from hamster brain. Here we demonstrate by CD and tryptophan (Trp) fluorescence spectroscopy that copper induces changes to the tertiary structure of SHaPrP(29−231). Binding of copper quenches the Trp fluorescence emission significantly, shifts the emission spectrum to shorter wavelengths, and also induces changes in the near-UV CD spectrum of SHaPrP(29−231). The binding sites are highly specific for $Cu^{2+}$, as indicated by the lack of a change in Trp fluorescence emission with $Ca^{2+}$, $Co^{2+}$, $Mg^{2+}$, $Mn^{2+}$, $Ni^{2+}$, and $Zn^{2+}$. Binding of $Cu^{2+}$ also promotes the conformational shift from a predominantly α-helical to a *β*-sheet structure. Equilibrium dialysis experiments indicate a binding stoichiometry of ∼2 copper molecules per PrP molecule at physiologically relevant concentrations, and pH titration of $Cu^{2+}$ binding suggests a role for histidine as a chelating ligand. NMR spectroscopy has recently demonstrated that the octarepeats (PHGGGWGQ) in SHaPrP(29−231) lack secondary or tertiary structure in the absence of $Cu^{2+}$. Our results suggest that each $Cu^{2+}$ binds to a structure defined by two octarepeats (PHGGGWGQ) with one histidine and perhaps one glycine carbonyl chelating the ion. We propose that the binding of two copper ions to four octarepeats induces a more defined structure to this region.

Prions are the cause of neurodegenerative diseases in humans and other mammals (for review see refs *1* and *2*). These illnesses include Creutzfeldt−Jakob disease (CJD) in humans, scrapie of sheep, and bovine spongiform encephalopathy (BSE). Recent reports suggest that bovine prions can be transmitted to humans (*3*, *4*). In contrast to viruses and viroids, no nucleic acid genome is associated with prions. Infectious preparations of the prion protein (PrP)[1] are composed of a posttranslationally modified form ($PrP^{Sc}$) of the normal cellular isoform ($PrP^{C}$). No difference in the primary structure of these isoforms has been observed. However, spectroscopic studies revealed that $PrP^{C}$ has a high α-helical content, whereas $PrP^{Sc}$ is mainly composed of *β*-sheets (*5*, *6*). Prion replication requires the conversion of $PrP^{C}$ into $PrP^{Sc}$ where $PrP^{Sc}$ acts as a template and protein X functions as a chaperone for the process (*7*−*9*). Studies of prion replication at the cellular level reveal that both isoforms colocalize in caveolae-like domains, suggesting that conversion is likely to take place in these vesicles (*10*). Posttranslationally, $PrP^{C}$ is glycosylated at two Asp residues and is membrane anchored via a C-terminal glycosylphosphatidylinositol (GPI) anchor. The function of $PrP^{C}$ is unknown, and studies of mice deficient for PrP ($Prnp^{0/0}$) have failed to clarify its role (*11*−*14*).

A nearly full-length form of SHaPrP, SHaPrP(29−231), has been expressed in *Escherichia coli* and refolded to an α-helical conformation (*15*). Multidimensional NMR studies of SHaPrP(29−231) demonstrate that the N-terminal segment comprised of residues 29−124 is largely flexible, suggesting that PrP may normally bind a ligand or another protein to form a stable complex in vivo (*16*). Moreover, NMR data consistent with a highly flexible N-terminus have been reported for MoPrP(23−231) (*17*). As $PrP^{C}$ from hamster brain can be purified by $Cu^{2+}$ chelate chromatography (*5*), we considered $Cu^{2+}$ as a possible metal ion binding to PrP. Also, short peptides corresponding to the octapeptide repeat motif of PrP have been reported to bind $Cu^{2+}$ (*18*, *19*).

Disturbances in $Cu^{2+}$ homeostasis leading to dysfunction of CNS are well documented in humans and animals. In both Menkes and Wilson's diseases, CNS degeneration due to abnormalities in $Cu^{2+}$ metabolism occurs (*20*−*27*). Both diseases are recessive disorders in which serum $Cu^{2+}$ and ceruloplasmin levels are diminished. Menkes disease is manifest at birth and is due to a mutation of the MNK gene on the X chromosome while Wilson's disease appears in

†This work was supported by grants from the National Institutes of Health (NS14069, AG08967, AG02132, and NS22786). J.S. was supported by a postdoctoral fellowship from the Stipendienprogramm Infektionsforschung, Heidelberg.

* Address correspondence to this author. Phone: 415-476-4482. Fax: 415-476-8386.

‡ Department of Neurology.

⊥ Current address: Department of Cellular Biochemistry, Max-Planck-Institut für Biochemie, 82152 Martinsried, Germany.

§ Department of Cellular and Molecular Pharmacology.

|| Department of Biochemistry and Biophysics.

[1] Abbreviations: PrP, prion protein; $PrP^{C}$, cellular isoform of PrP; $PrP^{Sc}$, scrapie isoform of PrP; SHaPrP(29−231), recombinant Syrian hamster PrP residues 29−231; MES, 2-(*N*-morpholino)ethanesulfonic acid; APP, amyloid precursor protein; CD, circular dichroism.

S0006-2960(97)02827-4 CCC: $15.00 
Published on Web 05/02/1998

childhood and is due to a mutation of the WD gene on chromosome 13. Both the MNK and WD genes encode copper-transporting ATPases. In Wilson's disease, copper accumulates in the lenticular nuclei within the CNS, while in Menkes disease, copper deficiency causes widespread neuronal death and a reactive gliosis (*28*). In contrast to Menkes disease, Wilson's disease can be treated with copper chelating reagents. Interestingly, cuprizone, a $Cu^{2+}$ chelating reagent, has been used in mice to induce neuropathological changes similar to those found in the prion diseases. Cuprizone-treated mice develop spongiform degeneration and astrocytic gliosis reminiscent of that found in scrapie (*29, 30*).

In this paper, we demonstrate that an analogue of $PrP^C$, SHaPrP(29−231), binds two divalent copper ions at physiologically relevant concentrations. From studies of a long peptide derived from the PrP octarepeat regions, SHaPrP-(57−91), we propose that two octarepeats are capable of liganding each $Cu^{2+}$ and that $Cu^{2+}$ induces ordered structure in the regions of PrP(29−231) shown to be flexible by high-resolution NMR spectroscopy.

## MATERIALS AND METHODS

*SHaPrP(29−231) Expression, Purification, and Refolding.* Syrian hamster PrP consisting of residues 29−231 [SHaPrP-(29−231)] was expressed and purified as described previously for SHaPrP(90−231) (*15*). SHaPrP(29−231) was expressed in a protease-deficient *E. coli* strain (27C7) under control of the alkaline phosphatase promoter. The cells were homogenized by a microfluidizer (Microfluidics Corp.), and the insoluble fraction containing SHaPrP(29−231) was pelleted by centrifugation. The pellet was solubilized in 8-M GdnHCl and 100 mM DTT. SHaPrP(29−231) was purified by size exclusion chromatography in 6 M GdnHCl, 1 mM EDTA, and 50 mM Tris-HCl, pH 8, and subsequent reverse chromatography using a C4 column (Vydac) and an acetonitrile/water gradient. The pooled fractions containing SHaPrP were lyophilized, and SHaPrP was then solubilized in 8 M GdnHCl. For refolding, these samples were diluted to a final concentration of 100 $\mu$g/mL in 25 mM Tris−acetate, pH 8, and 5 mM EDTA. The solution was dialyzed against 20 mM sodium acetate, pH 5.5, and 0.05% $NaN_3$ and concentrated by ultrafiltration.

*Purification of $PrP^C$ from Hamster Brain.* A crude microsomal fraction of hamster brain was prepared, extracted with Zwittergent, and centrifuged as described (*5*). A metal chelating column loaded with $Cu^{2+}$ was used for further purification. The protein was eluted with 150 mM imidazole. Subsequently, the pooled $PrP^C$ fractions were immunopurified on a protein A column preloaded with the monoclonal antibody 3F4. Elution was performed with 0.1 M acetic acid, pH 3, and 0.15% Zwittergent. After neutralization with 1 M Tris-HCl, pH 8, the protein was concentrated by ultrafiltration (Centricon 30, Amicon). The final pH was 7.

*Preparation of SHaPrP(57−91) and SHaPrP(73−91).* The peptides containing residues 57−91 and 73−91 of SHaPrP were synthesized from amino acids protected by 9-fluorenylmethoxycarbonyl (Fmoc) on a Millipore (Bedford, MA) Model 950 Plus PepSynthesizer. The peptides were purified by reverse-phase high-performance liquid chromatography (HPLC). The fractions were lyophilized and resuspended.

*Preparation of Metal-Free PrP.* Refolded, concentrated SHaPrP(29−231) was dialyzed to 50 mM 2-(*N*-morpholino)-ethanesulfonic acid (MES), pH 6, and 0.05% $NaN_3$ containing 1 g/100 mL Chelex 100 (Bio-Rad) to remove trace amounts of metals. All buffers used were also Chelex treated and filtered. Flame absorption chromatography of SHaPrP-(29−231) and buffers showed no detectable $Cu^{2+}$ (<0.5 $\mu$M). After the final dialysis step, the protein concentration was determined spectrophotometrically at 280 nm. For SHaPrP-(29−231), an extinction coefficient (mg/mL) of 0.4012 was established by amino acid analysis (Protein Structure Laboratory, University of California, Davis).

*CD Spectroscopy.* CD spectra were collected on a Jasco 720 spectropolarimeter equipped with a stress plate modulator continuously purged with dry nitrogen. Calibration was carried out using (+)-10-camphorsulfonic acid in an aqueous solution. At least four spectra of the near- and far-UV range were accumulated, and the appropriate buffer blanks were subtracted. One centimeter cells were used for the collection of near-UV CD spectra and 0.1 and 0.05 cm cells for far-UV CD spectra. Unless stated otherwise, samples contained 50 mM MES, pH 6, and 0.05% $NaN_3$. The concentration of $SHaPrP^C$(29−231) was 6.7 $\mu$M. For the far-UV CD spectra a 4 $\mu$M protein concentration was used. Mean residue molar ellipticities (deg·$cm^2$/dmol) were calculated on the basis of the SHaPrP(29−231) concentration, the number of residues in the recombinant PrP molecule, and the cell path length. The secondary structure content was calculated by deconvolution of the amide CD spectra (*31*).

*Fluorescence Spectroscopy.* Fluorescence spectroscopy was carried out on a Perkin-Elmer LS 50B fluorospectrophotometer. Trp fluorescence emissions were collected following excitation at 280 nm at a SHaPrP(29−231) concentration of 1.68 $\mu$M, 50 mM MES, pH 6, and 0.05% $NaN_3$ in 5 mm microcuvettes. SHaPrP(29−231) contains eight Trp residues, six of which are within the octapeptide repeat region. To identify the contribution of the octarepeats to Trp fluorescence, similar studies were conducted with SHaPrP-(57−91) and SHaPrP(73−91), fragments containing four octarepeats and four tryptophans or two octarepeats and two tryptophans, respectively. SHaPrP(57−91) or SHaPrP(73−91) (2 $\mu$M) was incubated with different amounts of $CuCl_2$ in 50 mM MES, pH 6, and 0.05% $NaN_3$ for recording Trp fluorescence emissions.

For the titration and ion specificity experiments, increasing amounts of each metal ion were added and emission spectra collected. The emission intensity at the maximum (353 nm) was used to monitor metal binding.

Fluorescence spectra of SHaPrP(29−231) (1.5 $\mu$M) in the presence of different metals were also recorded at different pH values. The buffers used were 50 mM sodium acetate, pH 4.0 and 5.0, 50 mM MES, pH 6.0, and 50 mM 3-(*N*-morpholino)propanesulfonic acid (MOPS), pH 7.0. Experiments at higher pH values were not possible owing to the poor solubility of SHaPrP(29−231). At this concentration, aggregation begins around pH 7.0.

*Equilibrium Dialysis Experiments.* Experiments were performed using Teflon chambers (Sialomed) separated by a dialysis membrane with a 5 kDa molecular mass cutoff. On one side, 0.5 mL samples containing 2.5 $\mu$M SHaPrP-(29−231) in 25 mM MES, pH 6, 2 mM dodecyl maltoside, 0.05% $NaN_3$, and different amounts of $CuCl_2$ were placed.

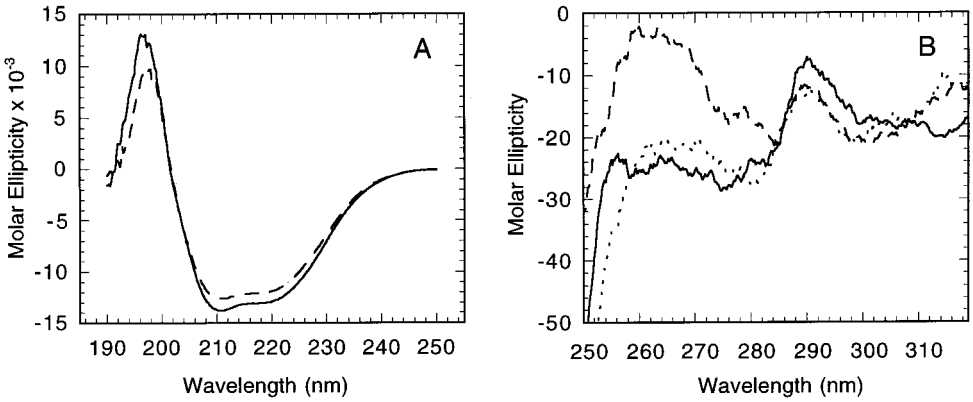


FIGURE 1: CD spectra of metal-free and copper-complexed SHaPrP(29−231). The near-UV CD spectra (A) indicate a mainly α-helical structure: (solid line) a metal-free preparation of SHaPrP(29−231) (4 $\mu$M) in 50 mM sodium acetate at pH 6 and (dashed line) after addition of 100 $\mu$M $CuCl_2$. The tertiary structure changes after addition of $Cu^{2+}$ (B): (solid line) metal-free SHaPrP(29−231) (6.7 $\mu$M) in 50 mM MES and 0.05% $NaN_3$ at pH 6 and (dashed line) after addition of 100 $\mu$M $CuCl_2$; (dotted line) purified $PrP^C$ from hamster brain (2.9 $\mu$M).

On the other side, 0.5 mL of a buffer solution of the corresponding $CuCl_2$ concentration was placed. To both samples a trace amount of $^{67}CuCl_2$ (Brookhaven National Laboratories) was added. For all experiments the protein concentration was kept constant and the $CuCl_2$ concentration was varied from 0.2 to 40 $\mu$M. The filled dialysis chambers were agitated for 48 h. This incubation time was sufficient to reach equilibrium if $^{67}CuCl_2$ was placed in only one chamber. Samples (400 $\mu$L) were withdrawn from each cell compartment, mixed with 5 mL of scintillation cocktail (Bio Safe II, Research Products International), and counted in a liquid scintillation counter (Beckmann LS7000). The fraction of the $CuCl_2$ solution bound was calculated according to the formula:

$$\text{fraction bound} = \frac{(\text{cpm}_{\text{PrPcompartment}} - \text{cpm}_{\text{CuCl}_2\text{compartment}})}{(\text{cpm}_{\text{PrPcompartment}} + \text{cpm}_{\text{CuCl}_2\text{compartment}})}$$

The $CuCl_2$ bound to PrP and the free $CuCl_2$ were calculated using the formulas:

$$[Cu^{2+}]_{\text{free}} = [Cu^{2+}]_{\text{total}} - [Cu^{2+}]_{\text{bound}}$$

and

$$[Cu^{2+}]_{\text{bound}} = [Cu^{2+}]_{\text{total}} \times \text{fraction bound}$$

*Heat Denaturation Experiments.* The influence of elevated temperatures on the secondary structure of SHaPrP(29−231) was monitored by CD at 222 nm. Preparations of SHaPrP-(29−231) (15 $\mu$M) in 25 mM sodium acetate, pH 6, were heated in 0.05 cm quartz cells with a programmable water circulator (Neslab 111). The $CuCl_2$ concentrations were 0, 25, 50, and 100 $\mu$M. The temperature was continuously increased (0.3 °C/min), and CD intensities were recorded in 0.1 °C increments. The signal at 25 °C was used to represent 100% folded α-helical protein, and the signal at 76 °C was used to represent 100% $\beta$-sheet aggregates. Data at other temperatures were normalized to these ellipticities to generate the fraction of denatured PrP. This shift of secondary structure was found to be irreversible upon cooling of the samples.

*Modeling of a Copper Binding Site in Human PrP.* A search through the Protein Data Bank (*32*) was made for both the octarepeat sequence from human PrP and the hexarepeat sequence from chicken PrP. A loop structure from sialidase (residues 547−552, sequence APGYPH) (*33*) was found to be homologous to the GPGYPH chicken hexarepeat. This structure was used as a template to model the human copper binding site, and $Cu^{2+}$ was placed in a square planar geometry. The structure was minimized and then validated with PROCHECK (*34*).

## RESULTS

*The Tertiary Structure of PrP Changes after Binding of Copper.* To study the metal binding properties of PrP, we used SHaPrP(29−231) expressed in *E. coli*. This construct lacks only the six N-terminal residues compared to mature $PrP^C$. After purification, SHaPrP(29−231) was refolded to an α-helical conformation (Figure 1A) that resembles the secondary structure of $PrP^C$ isolated from Syrian hamster brain (*5*). $PrP^C$ shows a near-UV CD spectrum comparable to the spectrum of metal-free SHaPrP(29−231) (Figure 1B). This suggests that recombinant, refolded PrP and the purified sample derived from hamster brain share similar secondary and tertiary structure.

Given the recurring presence of histidines in the PrP octarepeat region, we speculated that SHaPrP(29−231) would chelate divalent cations. To investigate $Cu^{2+}$ as a possible ligand for SHaPrP(29−231), we collected CD spectra in the absence and presence of $CuCl_2$. Metal-free and copper-complexed SHaPrP(29−231) show minima at 208 and 222 nm, which is indicative of a predominantly α-helical secondary structure. This is consistent with previous CD and more recent NMR studies of this molecule (*16*). The slight decrease in intensity after addition of $CuCl_2$ may suggest a minor unfolding of the molecule or an aggregation of PrP(29−231). The spectrum of the metal-free sample shows a prominent band at 295 nm. An additional band at 260 nm can be observed after addition of $CuCl_2$. This change in the aromatic region of the CD spectrum suggests a change of the tertiary structural environment of the aromatic residues in SHaPrP(29−231).

Trp fluorescence spectra of metal-free and $Cu^{2+}$-complexed preparations of SHaPrP(29−231) confirmed the

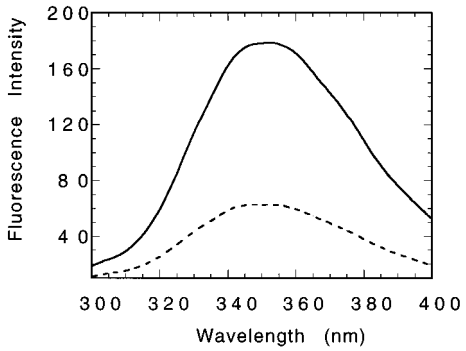


FIGURE 2: Trp fluorescence spectra of SHaPrP(29−231): (solid line) SHaPrP(29−231) (1.68 $\mu$M) in 50 mM MES and 0.05% $NaN_3$ at pH 6; (dashed line) the same preparation + 20 $\mu$M $CuCl_2$. The excitation wavelength was 280 nm. Addition of $CuCl_2$ quenches the emission intensity, and a second maximum at 347 nm is observed. Fluorescence intensities are given in arbitrary units.

observations made by CD spectroscopy. Addition of $CuCl_2$ induced a quench of the fluorescence to 30% of the initial intensity with the development of a shoulder on the original peak indicating a second maximum at 346.5 nm (Figure 2). This blue shift of the fluorescence signal suggests that the tryptophan indoles moved to a more hydrophobic environment. Similar studies of the isolated octarepeat region approximated by SHaPrP(57−91) show a comparable fluorescence quench (Figure 3A). As NMR studies of SHaPrP(29−231) and MoPrP(23−231) demonstrate that the octarepeat region is quite flexible (*16*, *17*), we suggest that $Cu^{2+}$ induces structure in the octarepeat region. However, there is no spectroscopic evidence to support the formation of the poly(L-proline) II structure suggested by work on isolated peptides (*35*).

*The Copper Binding Sites Are Saturable.* With Trp fluorescence spectroscopy we established that copper binding to SHaPrP(29−231) was saturable. SHaPrP(29−231) was incubated with different amounts of $CuCl_2$, and fluorescence emission spectra were recorded for each sample. At higher $Cu^{2+}$ concentrations, the fluorescence quench reached a plateau (Figure 3A). Half-maximal binding was reached at 14 $\mu$M $Cu^{2+}$. Since the titration curve is not truly sigmoidal, it is likely that SHaPrP(29−231) possesses nonidentical $Cu^{2+}$ binding sites with different dissociation constants. At copper concentrations above 30 $\mu$M, an additional decrease of the fluorescence signal was observed (see Figure 3D). This may be due to nonspecific binding and aggregation. Therefore, we limited analysis of the titration curve to copper concentrations below 30 $\mu$M. Similar titration curves were obtained using the peptides SHaPrP(57−91) and SHaPrP(73−91) (Figure 3A). The fluorescence intensity of SHaPrP(57−91) containing the octapeptide repeat region also reached a plateau at higher $CuCl_2$ concentrations (Figure 3A). This was also observed for SHaPrP(73−91), a PrP fragment containing only two octapeptide repeats. This allowed us to localize copper binding to the octapeptide repeat region and suggests that two consecutive octapeptides bind one $Cu^{2+}$ ion.

*The Binding Sites Are Specific.* To evaluate the specificity of the metal binding sites, we monitored the fluorescence intensity in the presence of a variety of divalent cations. SHaPrP(29−231) was incubated with $Ca^{2+}$, $Co^{2+}$, $Mg^{2+}$, $Mn^{2+}$, $Ni^{2+}$, and $Zn^{2+}$. Only copper induced a pronounced quench of fluorescence intensity (Figure 3B). No change of the Trp fluorescence signal was observed for the other cations used. To test the possibility that $Zn^{2+}$ and $Co^{2+}$ may bind at higher concentrations, samples of SHaPrP(29−231) were incubated with metal ions at concentrations up to 5 mM. Figure 3D depicts the Trp fluorescence intensity at different metal concentrations. The fluorescence emission was quenched only in the presence of $CuCl_2$, which demonstrates the high selectivity of the binding sites for copper.

*Copper Binding Is pH-Dependent.* To determine which amino acids are involved in complexing divalent cations, we incubated SHaPrP(29−231) with a variety of metal ions at different pH values and recorded Trp fluorescence emission for each sample. At pH 4, the fluorescence signal of the copper-complexed PrP sample did not differ from the metal-free sample (Figure 3C). At pH 5, a significant quench of the fluorescence signal of the copper-complexed sample was observed. This quench increased at pH 6 and 7. By contrast, the fluorescence emission spectra of metal-free PrP increased from pH 4 to pH 6 and slightly decreased from pH 6 to pH 7. The observation that binding titrates around pH 6 suggests that histidine plays a role in complexing $Cu^{2+}$. Each octarepeat contains one histidine. In SHaPrP(29−231), five histidine residues are located in the octarepeat region, which suggests that this domain of the protein could bind one, two, or five $Cu^{2+}$ molecules depending upon the number of imidazole ligands per $Cu^{2+}$. The fluorescence signal at 353 nm for all of the other metals did not differ from the metal-free PrP sample. This confirms the specificity of the ligand binding sites.

*Equilibrium Dialysis Experiments.* We performed equilibrium dialysis experiments to demonstrate binding directly, to calculate the number of binding sites, and to obtain the $Cu^{2+}$ dissociation constants. Trace amounts of $^{67}CuCl_2$ were used to measure the copper concentration in each dialysis chamber. Figure 4 shows the amount of $Cu^{2+}$ bound per mole of SHaPrP(29−231) plotted versus the copper concentration. The binding curve corresponds well to the data obtained by Trp fluorescence spectroscopy. Saturation is indicated by the plateau at higher copper concentrations. For SHaPrP(29−231), saturation was reached at ~1.8 $Cu^{2+}$ ions per SHaPrP(29−231) molecule. Half-saturation was observed for 14 $\mu$M $Cu^{2+}$. This suggests that SHaPrP(29−231) possesses two binding sites specific for $Cu^{2+}$ with a dissociation constant of 14 $\mu$M.

*Copper Binding Increases the Tendency To Form $\beta$-Sheet Aggregates.* Although attempts to convert recombinant PrP and its fragments into infectious $PrP^{Sc}$ have failed, previous studies have demonstrated that PrP and its fragments can be transformed from a predominantly α-helical monomeric form to an oligomeric $\beta$-sheet-rich state (*36*, *37*). SHaPrP(29−231) can also be converted from a mainly α-helical form to a $\beta$-sheet-rich structure upon heating. Metal-free SHaPrP(29−231) has a predominantly α-helical secondary structure as shown by CD spectroscopy (Figures 1A and 5B). Deconvolution of these spectra yields 32% α-helix and 12% $\beta$-sheet content. These results correlate well with NMR studies for the helical component (29% = 58/203) but overestimate the $\beta$-sheet contribution (<4% ≤ 8/203) (*16*). After the sample was heated to 76 °C, the CD spectrum showed a minimum at 217 nm, indicating a higher $\beta$-sheet

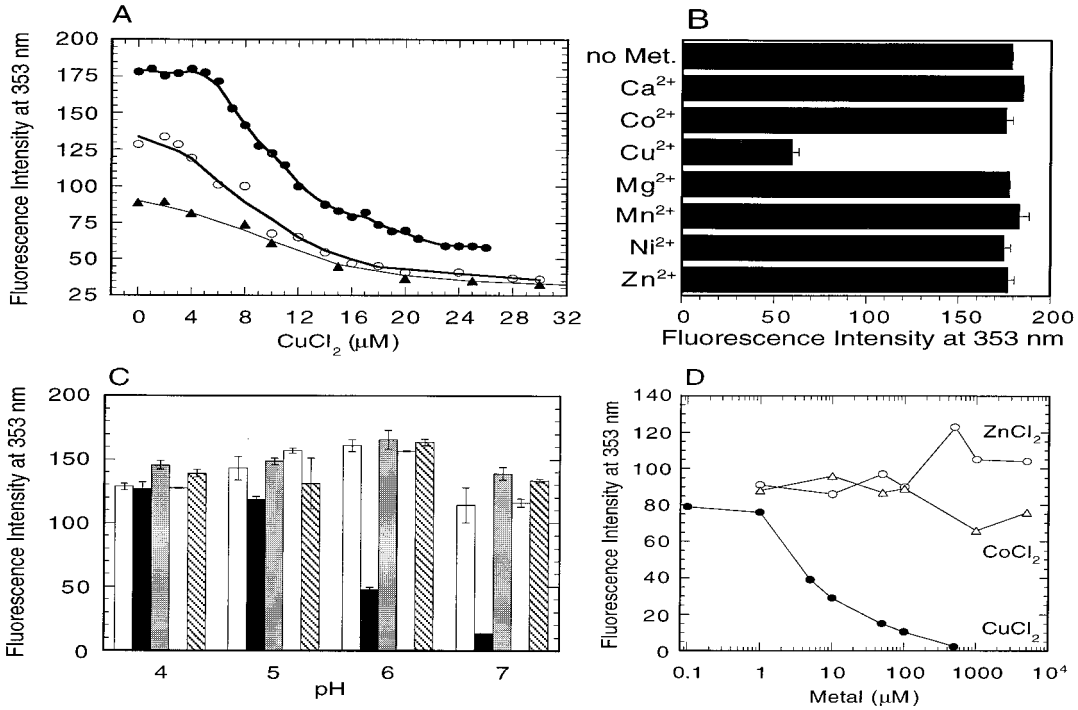


FIGURE 3: Metal binding to recombinant SHaPrP(29−231) as well as to synthesized SHaPrP(57−91) and SHaPrP(73−91) monitored by Trp fluorescence. $Cu^{2+}$ binding to SHaPrP(29−231) is specific and saturable. (A) The fluorescence signals of SHaPrP(29−231) (1.68 $\mu$M) (solid circles), SHaPrP(57−91) (2 $\mu$M) (open circles), and SHaPrP(73−91) (2 $\mu$M) (solid triangles) after addition of increasing amounts of $CuCl_2$. The samples were in 50 mM MES and 0.05% $NaN_3$ at pH 6. (B) Quenching of the Trp fluorescence intensity is observed only with $CuCl_2$. The fluorescence emission intensity at 353 nm of SHaPrP(29−231) was measured after incubation with 20 $\mu$M amounts of various metals. The first bar shows the fluorescence intensity of a control sample without metal addition. The error bars represent the standard error ($n = 2$). (C) The quench of fluorescence occurs around pH 6 and is specific for copper at different pH values. SHaPrP(29−231) (1.5 $\mu$M) was incubated at different pH values (for buffers see Materials and Methods) with 20 $\mu$M amounts of different metals, and the fluorescence intensity at 353 nm was measured. The bars represent, from left to right, metal-free SHaPrP(29−231) and the same preparation after addition of $CuCl_2$, $ZnCl_2$, $CoCl_2$, and $MnCl_2$. The error bars represent the standard error ($n \geq 3$). (D) The decrease of the fluorescence signal is not observed for $ZnCl_2$ or $CoCl_2$ up to concentrations of 5 mM. The experiment presented was performed as in (A). The concentration of SHaPrP(29−231) was 1 $\mu$M. Fluorescence intensities are shown in arbitrary units.

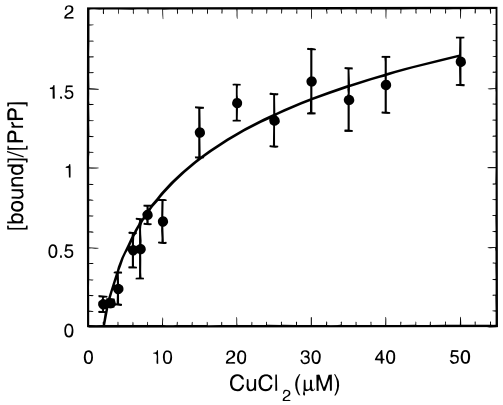


FIGURE 4: Binding of $CuCl_2$ to SHaPrP(29−231) measured by equilibrium dialysis experiments. Equilibrium dialysis of SHaPrP-(29−231) was performed as described in Materials and Methods. The maximal molar ratio of $Cu^{2+}$ to SHaPrP(29−231) found is ~1.8. The half-maximal binding observed for SHaPrP(29−231) is 14 $\mu$M. The error bars represent the standard error ($n \geq 5$).

content (Figure 5B, 1% α-helix and 38% $\beta$-sheet). This shift to a $\beta$-rich structure was not reversible upon cooling. The CD spectrum obtained after the sample was cooled from 76 to 25 °C indicates an intermediate secondary structure between the α-helical state after refolding and the more $\beta$-sheet-rich structure at 76 °C. Figure 5A shows the loss of helical secondary structure monitored by CD spectroscopy at 222 nm. For metal-free SHaPrP(29−231), thermal changes began at 45 °C and reached a plateau at 74 °C. The transition is cooperative with a midpoint at 60 °C. Addition of 25 $\mu$M $CuCl_2$ ($CuCl_2$/PrP ratio of 1.7) did not influence this change of structure significantly. After the $CuCl_2$ concentration was increased to 50 $\mu$M, a probable supraphysiologic concentration, copper-complexed SHaPrP(29−231) ($CuCl_2$/PrP ratio of 2.3) showed a similar cooperative change of secondary structure. However, the curve showing the temperature-dependent change of secondary structure was shifted to lower temperatures with a transition midpoint of 56 °C (Figure 5A). Similar behavior is seen at 100 $\mu$M $CuCl_2$. Figure 5C depicts the CD spectra of copper-complexed SHaPrP(29−231) (100 $\mu$M $CuCl_2$) recorded at 25 and 76 °C and after the sample was cooled from 76 to 25 °C. At 25 °C, the spectrum shows two minima at 208 and 222 nm, which are typical for an α-helical conformation. After the sample was heated to 76 °C, a decrease of the signal intensity and a minimum at 217 nm is observed, indicating the emergence of a $\beta$-sheet structure. This change of secondary structure was not reversible upon cooling of the samples. Between 25 and 50 $\mu$M $CuCl_2$, the midpoint of the change of secondary structure shifted to a lower temperature. In addition, the $\beta$-sheet structure achieved by heating the sample becomes more stable. That is, the shift is less reversible. Binding of $Cu^{2+}$ promotes the change of secondary structure of SHaPrP(29−231).

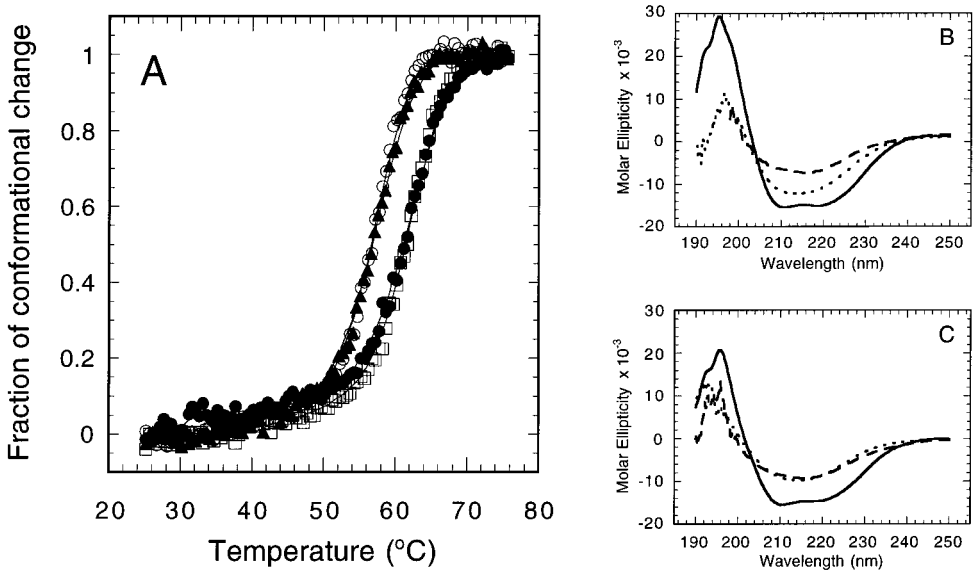


FIGURE 5: Binding of $CuCl_2$ increases the tendency of SHaPrP(29−231) to form $\beta$-sheet aggregates. Samples of SHaPrP(29−231) (15 $\mu$M) in 25 mM sodium acetate, pH 6, without and with 25, 50, and 100 $\mu$M $CuCl_2$, were heated from 25 to 76 °C. The shift of the mainly α-helical secondary structure to a $\beta$-sheet structure was monitored by CD spectroscopy. (A) The CD signal at 222 nm was recorded with increasing temperature. The metal-free sample (solid circles) and the samples containing 25 (open squares), 50 (open circles), and 100 $\mu$M (solid triangles) $CuCl_2$ show transition midpoints at 60, 60, 56, and 56 °C, respectively. (B) CD spectra of metal-free SHaPrP(29−231) at 25 °C (solid line), at 76 °C (dashed line), and after cooling from 76 to 25 °C (dotted line). (C) CD spectra of SHaPrP(29−231) after addition of 100 $\mu$M $CuCl_2$ at 25 °C (solid line) and 76 °C (dashed line) and after cooling from 76 to 25 °C (dotted line).

## DISCUSSION

The results presented herein demonstrate that PrP possesses $Cu^{2+}$-specific metal binding sites. Binding monitored by Trp fluorescence quenching and direct evidence from equilibrium dialysis both give an average dissociation constant of 14 $\mu$M. Is this a physiologically relevant binding site? The reported copper concentration in human serum is in the 10−25 $\mu$M range (*28*). Compared to other tissues, the copper concentration in the brain has been reported to be relatively high, 23.9 and 22.5 $\mu$g/g dry weight (*38*, *39*, *45*). On the basis of the water content of human tissues (*40*), the average copper concentration in human brain is about 80 $\mu$M. Interestingly, the total copper content of different brain regions varies widely (*41*); the highest values are found in the *locus ceruleus* (1.3 mM) and in the *substantia nigra* (0.4 mM). Although the precise free copper concentration in the brain is not known, our data indicate that PrP could be copper complexed in vivo.

Adding to the possible physiologic relevance of $Cu^{2+}$ binding to PrP is the specificity of the binding sites for $Cu^{2+}$ over other divalent cations. We observed no significant difference in Trp fluorescence intensity upon the addition of comparable concentrations of other divalent cations. Even at much higher concentrations, $Zn^{2+}$ and $Co^{2+}$ do not induce a quench of the fluorescence intensity. There are some unique features of the coordination of $Cu^{2+}$ in proteins: $Cu^{2+}$ prefers octahedral or square planar coordination while $Zn^{2+}$ and $Co^{2+}$ normally adopt a tetrahedral coordination geometry (*42*). Other metals that prefer octahedral or square planar coordination such as $Ag^{3+}$ were not studied due to technical reasons.

The equilibrium dialysis experiments indicate two (∼1.8) $Cu^{2+}$ binding sites for SHaPrP(29−231). Binding of copper to peptides containing the highly conserved octapeptide repeat (PHGGGWGQ) has been reported (*18*, *19*). Copper binding to these octarepeat-containing peptides was shown by mass spectrometry and size exclusion chromatography (*18*). The ratio between the number of octapeptide repeats and the number of $Cu^{2+}$ ions bound was not clarified. Fourier transformation infrared spectroscopy indicates a copper induced α-helix formation in these peptides (*19*). Since these studies were performed with short peptides, it is difficult to apply the results to full-length PrP. Using a longer peptide, SHaPrP(57−91), we observed a quench of the Trp fluorescence comparable to SHaPrP(29−231), which argues that copper binding takes place in this region. Although the octapeptide repeat region is not required for the infectivity of $PrP^{Sc}$, this octapeptide repeat region is highly conserved between species, which suggests an important role in the normal function of the protein (*43*, *44*). NMR studies of SHaPrP(29−231) show that, in the apoprotein, the octarepeat peptide region is mainly unstructured and flexible (*16*, *17*). While the binding of copper might induce a tertiary structure in this region, NMR studies of this structure will be complicated because of the paramagnetic properties of $Cu^{2+}$.

The pH titration and peptide fragment experiments suggest that the imidazole side chains of histidines in the octarepeat peptide region are involved in chelating the $Cu^{2+}$ ions, and the pronounced quench of Trp fluorescence is presumably due to the close proximity of Trp residues to the copper binding site. Within each octarepeat, the His and Trp residues are separated by three Gly residues and the Trp is bounded on the N-terminal side by a fourth Gly. To model the human copper binding site, a search through the Protein Data Bank (*32*) was made for both the octarepeat sequence from human PrP and the hexarepeat sequence from chicken PrP. A loop structure from sialidase (residues 547−552, sequence APGYPH) (*33*) was found to be homologous to the GPGYPH chicken hexarepeat. The Protein Data Bank

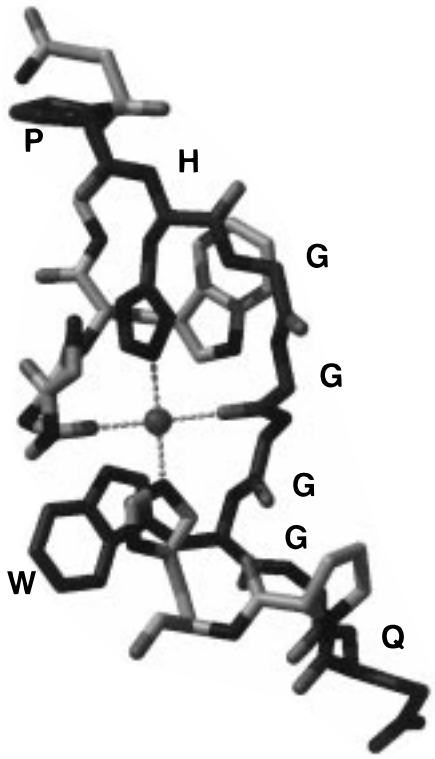


FIGURE 6: Possible conformation of $Cu^{2+}$ binding to two octapeptide repeats. Copper is coordinated by two His residues and two Gly carbonyl oxygens and is bound in a square planar geometry. Modeling was performed using the Sybyl software package (Tripos Inc.), and the structure was validated with PROCHECK (*34*). The color code is as follows: blue, nitrogen; red, oxygen; and green, copper.

also revealed that two residues in the sialidase hexapeptide, His and Gly, can play a role in Cu coordination (*45*). In this case, the Gly carboxyl oxygen is the ligand atom; the main chain N of Gly has also been found to ligate to $Cu^{2+}$ but only in the amino terminal "ATCUN" motif present in certain albumins (*46*). $Cu^{2+}$ induces a fluorescence quench in a PrP fragment containing two octarepeats, which suggests that one $Cu^{2+}$ ion is bound to two consecutive octapeptides. However, it is not clear whether a single $Cu^{2+}$ binds to two consecutive or two nonconsecutive octarepeats. It was possible to form a planar tetrahedral $Cu^{2+}$ binding site by fusing two chicken hexapeptides and by using the His NE2 and Gly carboxyl oxygen C-terminal of the Pro as ligands for $Cu^{2+}$. This structure was used as a template to model the human copper binding site. There are four Gly residues in the human octarepeat; since the Gly directly N-terminal of the Trp is mutated to a Ser in mouse PrP, it can be discounted as a potential $Cu^{2+}$ ligand. Models were constructed using the other three Gly residues in the octapeptides as potential ligands. The location of the proline, the presumed symmetry of the site, and the geometric properties of the $Cu^{2+}$−histidine, carbonyl, histidine, carbonyl coordination complex were specified. The Gly carboxyl oxygen in the middle of the Gly triplet in the octapeptide was chosen as the ligand because this enabled the Trp to come into proximity with the $Cu^{2+}$ center and can account for the Trp fluorescence quenching upon binding of $Cu^{2+}$ to PrP(29−231). This structure was validated with PROCHECK (*34*) (Figure 6).

Since NMR studies of the $Cu^{2+}$-complexed protein will be challenging, more accurate models of the structure of this region must await crystallographic studies. Whether the in vivo function of $PrP^{C}$ involves the binding, transport, or metabolism of $Cu^{2+}$ ions remains to be established. A loss of cerebellar Purkinje cells has been reported for one line of older mice deficient for PrP ($Prnp^{0/0}$) (*47*); however, this phenotype was not seen in other lines of $Prnp^{0/0}$ mice (*11*). Altered circadian rhythms and sleep patterns were found in two lines of $Prnp^{0/0}$ mice (*14*).

Our findings raise the possibility that copper binding plays a role in the function of PrP. While the dissociation constant is rather high compared to other protein−metal interactions, it is in the range of the available copper concentration in the brain. Thus, $PrP^{C}$ might function as a copper sensor. Interestingly, the Cu/Zn superoxide dismutase activity was found to be reduced in the brains of $Prnp^{0/0}$ mice, and cultured cells derived from brains of these mice were observed to be more sensitive to oxidative stress (*48*). The level of Cu/Zn dismutase activity is thought to reflect copper status in different tissues. Restriction of copper in the diet of animals leads to a decrease of Cu/Zn superoxide dismutase activity. Administration of $CuCl_2$ to these animals restores activity (for a review see ref *49*). These findings raise the possibility that PrP is involved in the supply or regulation of $Cu^{2+}$ in the brain. PrP might also act as a sink for free copper to minimize the generation of oxygen radicals catalyzed by copper ions (Fenton reaction). Additional evidence for an involvement of copper in the pathogenesis of prion diseases comes from studies where cuprizone, a $Cu^{2+}$ chelating reagent (*50*), was administered to mice. Cuprizone induced pathological changes in the brains of mice comparable to those found in scrapie-infected mice (*29*, *30*).

Whether $PrP^{Sc}$ binds $Cu^{2+}$ and whether such binding or lack thereof features in the neurodegeneration of prion disease are unknown. The binding of metal ions to the A$\beta$ peptide proteolytically derived from APP has been suggested to feature in the pathogenesis of another neurodegenerative disorder, Alzheimer's disease (*51*). Human A$\beta$ contains two binding sites for $Zn^{2+}$, and concentrations of $Zn^{2+}$ above 300 nM induce a shift in secondary structure where A$\beta$ aggregates into amyloid in the presence of $Zn^{2+}$ more readily (*52*). Recently, a copper binding site was reported for APP and the reduction of $Cu^{2+}$ to $Cu^{+}$ by APP, was proposed to play a role in the neurodegeneration of Alzheimer's disease (*53*).

To gain information about differences between metal-free and copper-complexed PrP, we performed heat denaturation experiments. Copper-complexed PrP is more prone to shift from a soluble, primarily $\alpha$-helical structure to a $\beta$-sheet aggregate. This change in secondary structure is shifted to a lower temperature and is less reversible in the presence of bound copper. Thus, the binding of copper facilitates thermodynamically the formation of a $\beta$-sheet aggregate. Since the mechanism of prion diseases involves a comparable change of conformation, this raises the possibility that the binding of copper features in $PrP^{Sc}$ formation or the pathogenic process. Interestingly, in some cases of inherited CJD additional octarepeat sequences are inserted in one PrP allele (*54*−*56*). A disturbance of copper binding in these extended PrP proteins might participate in the pathogenesis of these familial CJD cases. It is notable that the deletion of one octapeptide repeat does not trigger disease. Whether

copper influences the formation of a conversion-competent form, designated PrP*, or a complex of PrP* and another protein needed for the conversion, protein X (*8*, *9*), remains to be determined. Binding of copper might also modify the second step of the conversion reaction where the activated PrP* sandwiched between protein X and $PrP^{Sc}$ is transformed into a nascent $PrP^{Sc}$ molecule.

## ACKNOWLEDGMENT

We thank Darlene Groth, Patrick Culhane, and Ingrid Mehlhorn for the purification of SHaPrP(29−231); Hana Serban for purification of $PrP^{C}$ from hamster brain; and Haydn Ball, Tatiana Bekker, and Michael Baldwin for the synthesis and purification of SHaPrP(57−91) and SHaPrP-(73−91).

## REFERENCES

1. Prusiner, S. B. (1991) *Science 252*, 1515−1522.
2. Prusiner, S. B. (1997) *Science 278*, 245−251.
3. Chazot, G., Broussolle, E., Lapras, C. I., Blättler, T., Aguzzi, A., and Kopp, N. (1996) *Lancet 347*, 1181.
4. Will, R. G., Ironside, J. W., Zeidler, M., Cousens, S. N., Estibeiro, K., Alperovitch, A., Poser, S., Pocchiari, M., Hofman, A., and Smith, P. G. (1996) *Lancet 347*, 921−925.
5. Pan, K.-M., Baldwin, M., Nguyen, J., Gasset, M., Serban, A., Groth, D., Mehlhorn, I., Huang, Z., Fletterick, R. J., Cohen, F. E., and Prusiner, S. B. (1993) *Proc. Natl. Acad. Sci. U.S.A. 90*, 10962−10966.
6. Safar, J., Roller, P. P., Gajdusek, D. C., and Gibbs, C. J., Jr. (1993) *J. Biol. Chem. 268*, 20276−20284.
7. Cohen, F. E., Pan, K.-M., Huang, Z., Baldwin, M., Fletterick, R. J., and Prusiner, S. B. (1994) *Science 264*, 530−531.
8. Kaneko, K., Zulianello, L., Scott, M., Cooper, C. M., Wallace, A. C., James, T. L., Cohen, F. E., and Prusiner, S. B. (1997) *Proc. Natl. Acad. Sci. U.S.A. 94*, 10069−10074.
9. Telling, G. C., Scott, M., Mastrianni, J., Gabizon, R., Torchia, M., Cohen, F. E., DeArmond, S. J., and Prusiner, S. B. (1995) *Cell 83*, 79−90.
10. Vey, M., Pilkuhn, S., Wille, H., Nixon, R., DeArmond, S. J., Smart, E. J., Anderson, R. G., Taraboulos, A., and Prusiner, S. B. (1996) *Proc. Natl. Acad. Sci. U.S.A. 93*, 14945−14949.
11. Büeler, H., Fischer, M., Lang, Y., Bluethmann, H., Lipp, H.-P., DeArmond, S. J., Prusiner, S. B., Aguet, M., and Weissmann, C. (1992) *Nature 356*, 577−582.
12. Collinge, J., Whittington, M. A., Sidle, K. C., Smith, C. J., Palmer, M. S., Clarke, A. R., and Jefferys, J. G. R. (1994) *Nature 370*, 295−297.
13. Lledo, P.-M., Tremblay, P., DeArmond, S. J., Prusiner, S. B., and Nicoll, R. A. (1996) *Proc. Natl. Acad. Sci. U.S.A. 93*, 2403−2407.
14. Tobler, I., Gaus, S. E., Deboer, T., Achermann, P., Fischer, M., Rülicke, T., Moser, M., Oesch, B., McBride, P. A., and Manson, J. C. (1996) *Nature 380*, 639−642.
15. Mehlhorn, I., Groth, D., Stöckel, J., Moffat, B., Reilly, D., Yansura, D., Willett, W. S., Baldwin, M., Fletterick, R., Cohen, F. E., Vandlen, R., Henner, D., and Prusiner, S. B. (1996) *Biochemistry 35*, 5528−5537.
16. Donne, D. G., Viles, J. H., Groth, D., Mehlhorn, I., James, T. L., Cohen, F. E., Prusiner, S. B., Wright, P. E., and Dyson, H. J. (1997) *Proc. Natl. Acad. Sci. U.S.A. 94*, 13452−13457.
17. Riek, R., Hornemann, S., Wider, G., Glockshuber, R., and Wüthrich, K. (1997) *FEBS Lett. 413*, 282−288.
18. Hornshaw, M. P., McDermott, J. R., Candy, J. M., and Lakey, J. H. (1995) *Biochem. Biophys. Res. Commun. 214*, 993−999.
19. Miura, T., Hori-i, A., and Takeuchi, H. (1996) *FEBS Lett. 396*, 248−252.
20. Bull, P. C., Thomas, G. R., Rommens, J. M., Forbes, J. R., and Cox, D. W. (1993) *Nat. Genet. 5*, 327−337.
21. Chelly, J., Tümer, Z., Tønnesen, T., Petterson, A., Ishikawa-Brush, Y., Tommerup, N., Horn, N., and Monaco, A. P. (1993) *Nat. Genet. 3*, 14−19.
22. Levinson, B., Vulpe, C., Elder, B., Martin, C., Verley, F., Packman, S., and Gitschier, J. (1994) *Nat. Genet. 6*, 369−373.
23. Mercer, J. F. B., Livingston, J., Hall, B., Paynter, J. A., Begy, C., Chandrasekharappa, S., Lockhart, P., Grimes, A., Bhave, M., Siemieniak, D., and Glover, T. W. (1993) *Nat. Genet. 3*, 20−25.
24. Petrukhin, K., Fischer, S. G., Pirastu, M., Tanzi, R. E., Chernov, I., Devoto, M., Brzustowicz, L. M., Cayanis, E., Vitale, E., Russo, J. J., Matseoane, D., Boukhgalter, B., Wasco, W., Figus, A. L., Loudianos, J., Cao, A., Sternlieb, I., Evgrafov, O., Parano, E., Pavone, L., Warburton, D., Ott, J., Penchaszadeh, G. K., Scheinberg, I. H., and Gilliam, T. C. (1993) *Nat. Genet. 5*, 338−343.
25. Tanzi, R. E., Petrukhin, K., Chernov, I., Pellequer, J. L., Wasco, W., Ross, B., Romano, D. M., Parano, E., Pavone, L., Brzustowicz, L. M., Devoto, M., Peppercorn, J., Bush, A. I., Sternlieb, I., Pirastu, M., Gusella, J. F., Evgrafov, O., Penchaszadeh, G. K., Honig, B., Edelman, I. S., Soares, M. B., Scheinberg, I. H., and Gilliam, T. C. (1993) *Nat. Genet. 5*, 344−350.
26. Vulpe, C., Levinson, B., Whitney, S., Packman, S., and Gitschier, J. (1993) *Nat. Genet. 3*, 7−13.
27. Wu, J., Forbes, J. R., Chen, H. S., and Cox, D. W. (1994) *Nat. Genet. 7*, 541−545.
28. Danks, D. M. (1989) in *The Metabolic Basis of Inherited Disease* (Scriber, C. R., Beaudet, A. L., Sly, W. S., and Valle, D., Eds.) 6th ed., pp 1411−1462, McGraw-Hill, Inc., New York.
29. Kimberlin, R. H., Millson, G. C., Bountiff, L., and Collis, S. C. (1974) *J. Comput. Pathol. 84*, 263−270.
30. Pattison, I. H., and Jebbett, J. N. (1971) *Res. Vet. Sci. 12*, 378−380.
31. Sreerama, N., and Woody, R. W. (1993) *Anal. Biochem. 209*, 32−44.
32. Bernstein, F. C., Keotzle, T. F., Williams, G. J. B., Meyer, E. F., Jr., Brice, M. D., Rodgers, J. R., Kennard, O., Shimanouchi, T., and Tasumi, M. (1977) *J. Mol. Biol. 112*, 535−542.
33. Gaskell, A., Crennell, S., and Taylor, G. (1995) *Structure 3*, 1197−1205.
34. Laskowski, R. A., MacArthur, M. W., Moss, D. S., and Thornton, J. M. (1993) *J. Appl. Crystallogr. 26*, 283−291.
35. Smith, C. J., Drake, A. F., Banfield, B. A., Bloomberg, G. B., Palmer, M. S., Clarke, A. R., and Collinge, J. (1997) *FEBS Lett. 405*, 378−384.
36. Zhang, H., Kaneko, K., Nguyen, J. T., Livshits, T. L., Baldwin, M. A., Cohen, F. E., James, T. L., and Prusiner, S. B. (1995) *J. Mol. Biol. 250*, 514−526.
37. Zhang, H., Stöckel, J., Mehlhorn, I., Groth, D., Baldwin, M. A., Prusiner, S. B., James, T. L., and Cohen, F. E. (1997) *Biochemistry 36*, 3543−3553.
38. Iyengar, G. V., Kollmer, W. E., and Bowen, H. J. M. (1978) *The elemental composition of human tissues and body fluids: a compilation of values for adults*, Verlag Chemie, New York, NY.
39. Smith, H. (1967) *J. Forens. Sci. Soc. 7*, 97−102.
40. Hamilton, E. I., Minski, M. J., and Cleary, J. J. (1972/1973) *Sci. Total Environ. 1*, 341−374.
41. Smith, R. M. (1983) in *Neurobiology of the trace elements* (Dreosti, I. E., and Smith, R. M., Eds.) pp 1−39, Humana Press, Clifton, NJ.
42. Glusker, J. P. (1991) *Adv. Protein Chem. 42*, 1−76.
43. Bamborough, P., Wille, H., Telling, G. C., Yehiely, F., Prusiner, S. B., and Cohen, F. E. (1996) *Cold Spring Harbor Symp. Quant. Biol. 61*, 495−509.
44. Schätzl, H. M., Da Costa, M., Taylor, L., Cohen, F. E., and Prusiner, S. B. (1995) *J. Mol. Biol. 245*, 362−374.
45. Nar, H., Messerschmidt, A., and Huber, R. (1991) *J. Mol. Biol. 218*, 427−447.

46. Harford, C., and Sarkar, B. (1997) *Acc. Chem. Res. 30*, 123−130.
47. Sakaguchi, S., Katamine, S., Nishida, N., Moriuchi, R., Shigematsu, K., Sugimoto, T., Nakatani, A., Kataoka, Y., Houtani, T., Shirabe, S., Okada, H., Hasegawa, S., Miyamoto, T., and Noda, T. (1996) *Nature 380*, 528−531.
48. Brown, D. R., Schulz-Schaeffer, W. J., Schmidt, B., and Kretzschmar, H. A. (1997) *Exp. Neurol. 146*, 104−112.
49. Harris, E. D. (1992) *J. Nutr. 122*, 636−640.
50. Rohde, R. K. (1966) *Anal. Chem. 38*, 911−913.
51. Selkoe, D. J. (1994) *J. Neuropathol. Exp. Neurol. 53*, 438−447.
52. Bush, A. I., Pettingell, W. H., Multhaup, G., Paradis, M. d., Vonsattel, J.-P., Gusella, J. F., Beyreuther, K., Masters, C. L., and Tanzi, R. E. (1994) *Science 265*, 1464−1467.
53. Multhaup, G., Schlicksupp, A., Hesse, L., Beher, D., Ruppert, T., Masters, C. L., and Beyreuther, K. (1996) *Science 271*, 1406−1409.
54. Goldfarb, L. G., Brown, P., McCombie, W. R., Goldgaber, D., Swergold, G. D., Wills, P. R., Cervenakova, L., Baron, H., Gibbs, C. J. J., and Gajdusek, D. C. (1991) *Proc. Natl. Acad. Sci. U.S.A. 88*, 10926−10930.
55. Owen, F., Poulter, M., Lofthouse, R., Collinge, J., Crow, T. J., Risby, D., Baker, H. F., Ridley, R. M., Hsiao, K., and Prusiner, S. B. (1989) *Lancet 1*, 51−52.
56. Poulter, M., Baker, H. F., Frith, C. D., Leach, M., Lofthouse, R., Ridley, R. M., Shah, T., Owen, F., Collinge, J., Brown, G., Hardy, J., Mullan, M. J., Harding, A. E., Bennett, C., Doshi, R., and Crow, T. J. (1992) *Brain 115*, 675−685.

BI972827K